



Pre-clinical evaluation of antiviral activity of nitazoxanide against SARS-CoV-2

Jean-Sélim Driouich,^{a,*} Maxime Cochin,^a Franck Touret,^a Paul-Rémi Petit,^a Magali Gilles,^a Grégory Moureau,^a Karine Barthélémy,^a Caroline Laprie,^b Thanaporn Wattanakul,^c Palang Chotsiri,^c Richard M. Hoglund,^{c,d} Joel Tarning,^{c,d} Laurent Fraisse,^e Peter Sjö,^e Charles E. Mowbray,^e Fanny Escudié,^e Ivan Scandale,^e Eric Chatelain,^e Xavier de Lamballerie,^a Caroline Solas,^{a,f} and Antoine Nougairède^a

^aUnité des Virus Émergents (UVE: Aix-Marseille University -IRD 190-Inserm 1207), Marseille, France

^bLaboratoire Vet-Histo, Marseille, France

^cMahidol Oxford Tropical Medicine Research Unit, Faculty of Tropical Medicine, Mahidol University, Bangkok, Thailand

^dCentre for Tropical Medicine and Global Health, Nuffield Department of Clinical Medicine, University of Oxford, Oxford, United Kingdom

^eDrugs for Neglected Diseases initiative, Geneva, Switzerland

^fAPHM, Laboratoire de Pharmacocinétique et Toxicologie, Hôpital La Timone, Marseille, France

Summary

Background To address the emergence of SARS-CoV-2, multiple clinical trials in humans were rapidly started, including those involving an oral treatment by nitazoxanide, despite no or limited pre-clinical evidence of antiviral efficacy.

Methods In this work, we present a complete pre-clinical evaluation of the antiviral activity of nitazoxanide against SARS-CoV-2.

Findings First, we confirmed the *in vitro* efficacy of nitazoxanide and tizoxanide (its active metabolite) against SARS-CoV-2. Then, we demonstrated nitazoxanide activity in a reconstructed bronchial human airway epithelium model. In a SARS-CoV-2 virus challenge model in hamsters, oral and intranasal treatment with nitazoxanide failed to impair viral replication in commonly affected organs. We hypothesized that this could be due to insufficient diffusion of the drug into organs of interest. Indeed, our pharmacokinetic study confirmed that concentrations of tizoxanide in organs of interest were always below the *in vitro* EC₅₀.

Interpretation These preclinical results suggest, if directly applicable to humans, that the standard formulation and dosage of nitazoxanide is not effective in providing antiviral therapy for Covid-19.

Funding This work was supported by the Fondation de France “call FLASH COVID-19”, project TAMAC, by “Institut national de la santé et de la recherche médicale” through the REACTing (REsearch and ACTION targeting emerging infectious diseases), by REACTING/ANRS MIE under the agreement No. 21180 (‘Activité des molécules antivirales dans le modèle hamster’), by European Virus Archive Global (EVA 213 GLOBAL) funded by the European Union’s Horizon 2020 research and innovation program under grant agreement No. 871029 and DNDi under support by the Wellcome Trust Grant ref: 222489/Z/21/Z through the COVID-19 Therapeutics Accelerator”.

Copyright © 2022 The Author(s). Published by Elsevier B.V. This is an open access article under the CC BY license (<http://creativecommons.org/licenses/by/4.0/>)

Keywords: COVID-19; SARS-CoV-2; Antiviral therapy; Pre-clinical research; Nitazoxanide; Animal model

Introduction

The threat of a global pandemic caused by a virus from the *Coronaviridae* family, which are enveloped positive-sense single-stranded RNA viruses, has been hanging

over the whole world since the emergence of the severe acute respiratory syndrome coronavirus (SARS-CoV) and the Middle East respiratory syndrome (MERS-CoV). In December 2019, cases of pneumonia were reported in Wuhan, China.¹ Few months later, the causative agent was identified as a new betacoronavirus.² Named SARS-CoV-2, this pathogen progressed worldwide to such an extent that its disease, called coronavirus disease 2019 (COVID-19), was characterized as a pandemic

*Corresponding author.

E-mail address: jean-selim.driouich@univ-amu.fr (J.-S. Driouich).

Research in context

Evidence before this study

Nitazoxanide was one of the first compounds studied during the emergence of SARS-CoV-2. Today, numerous human clinical trials investigating the efficacy and safety of oral NTZ therapy are underway worldwide. However, preclinical evidence of antiviral efficacy is lacking or limited. On the one hand, there are currently no preclinical *in vivo* studies in the literature, and on the other hand, too few studies report on the pulmonary diffusion of this molecule.

Added value of this study

In the present study, we first confirmed the antiviral efficacy of NTZ and TIZ (its circulating active metabolite) *in vitro* before studying its activity against SARS-CoV-2 *in vivo*. However, NTZ failed to reduce the severity of SARS-CoV-2 infection *in vivo* in the Syrian hamster model: No improvement in clinical disease progression, viral replication and/or histopathological damage in the lungs was observed. The two pharmacokinetic studies (intra-organ dosing and modeling) that we performed, concluded that the pulmonary distribution of tizoxanide was insufficient. Therefore, the use of NTZ as an antiviral against SARS-CoV-2, does not seem appropriate at the current standard formulation and dosage.

Implications of all the available evidence

Our results suggest that the low pulmonary bioavailability of NTZ remains the major challenge that needs to be addressed in order to properly evaluate the potential antiviral effect of NTZ in animal model and/or in clinical trials.

by the World Health Organization on March 2020.³ COVID-19 leads to a broad spectrum of clinical syndromes, ranging from pauci-symptomatic disease to severe pneumonia and acute respiratory distress syndrome.⁴ As a concerted effort between governments, scientists, businesses, civil society and global health organizations including Wellcome, Unitaaid and BMGF, the Access to COVID-19 Tools (ACT) Accelerator partnership was launched in April 2020. The collaboration is articulated around four pillars and aim to provide a global solution by accelerating development, production, and equitable access to COVID-19 tests, treatments, and vaccines widely including in LMICs. In this context, the ANTICOV clinical trial was launched; its main objective is to conduct an open-label, multicenter, randomized, adaptive platform trial to test the safety and efficacy of several marketed products, including antiviral therapies versus control in mild/moderate of coronavirus disease 2019 (Covid-19) in resource-limited-settings. Its aim is thereby to prevent spikes in hospitalizations that could overwhelm fragile and already

overburdened health systems in low- and middle-income countries. Thus, repurposed drugs, such as NTA, have been considered as an interesting strategy to identify active antiviral therapy against SARS-CoV-2.

Nitazoxanide (NTZ) was originally developed as an antiprotozoal agent and marketed for the treatment of *Giardia* and *Cryptosporidium* infections. In recent years, it was identified as a broad-spectrum antiviral drug.^{5–7} NTZ, and its active circulating metabolite, tizoxanide (TIZ), inhibit the replication of a wide range of RNA and DNA viruses in cell culture assays including hepatitis B, hepatitis C, rotavirus, norovirus, dengue, yellow fever, Japanese encephalitis virus and the human immunodeficiency virus.^{6,8,9} Its inhibitory activity against viruses inducing respiratory infections was specifically investigated.¹⁰ Notably, NTZ possesses *in vitro* antiviral activity against influenza virus by blocking the maturation of the viral hemagglutinin, as well as against MERS coronavirus and other coronaviruses by inhibiting expression of the viral N protein.^{9,11–13}

It is thus quite naturally that this molecule was rapidly considered as a potential repurposing candidate for COVID-19 management.^{14–19} NTZ was one of the first molecules studied *in vitro* against SARS-CoV-2. One of the earliest studies on SARS-CoV-2 reported a 50% effective concentration (EC₅₀) of 2.12 μM in Vero E6 cells at 48 h post-infection.²⁰ Since then, several studies have confirmed this first evaluation and have reported EC₅₀ values ranging between 1.29 and 7.94 μM.^{9,21} Assumptions regarding the possible role of TIZ against numerous targets involved in SARS-CoV-2 pathogenesis affecting viral entry and multiplication were rapidly proposed. Additionally, recent findings have also demonstrated that NTZ could inhibit the TMEM16 protein, a calcium-activated ion channel involved in phospholipid transposition between the cell membranes, and block SARS-CoV-2-Spike induced syncytia.²² In addition, NTZ may have the capacity to boost host innate immune responses, affecting the well-described COVID-19 inflammatory cytokine storm. Ambitious expectations have also been raised about its potential ability to improve multi-organ damage and providing added value to patients with comorbidities.²³ Consequently, many clinical trials in human investigating the efficacy and the safety of an oral treatment of NTZ alone or in combination with other anti-SARS-CoV-2 candidates are ongoing worldwide (<https://clinicaltrials.gov/>; search terms: nitazoxanide|Covid19). Coverage Africa for example is a nested study in the large ANTICOV platform trial currently assessing the association of Ciclesonide/Nitazoxanide (total daily dose 2000 mg for 14 days) and the Telmisartan, compared with a control arm: paracetamol (NCT number: NCT04920838).

However, a full pre-clinical *in vivo* investigation of the activity of NTZ against SARS-CoV-2 had yet to be conducted. In the present study, we first confirmed the antiviral efficacy of NTZ and TIZ *in vitro* before

investigating activity against SARS-CoV-2 using reconstituted human airway epithelium and a previously described Syrian hamster model.^{24–26} A population pharmacokinetic model was developed to compare exposure in hamsters and humans, with the aim of assessing whether the exposure to NTZ and TIZ in preclinical animal species can be achieved in humans, and whether the antiviral potency observed *in vitro* can be recovered *in vivo*.

Methods

Cells and human airway epithelia

Vero E6 cells (ATCC CRL-1586, RRID:CVCL_0574) and Caco-2 cells (ATCC HTB-37, RRID:CVCL_0025) were cultivated under 5% CO₂ and at 37.5°C in minimal essential medium (MEM) supplemented with 7.5% heat-inactivated fetal bovine serum (FBS), 1% non-essential amino acids and 1% Penicillin/Streptomycin (all from Life Technologies). All cell lines were purchased from certified suppliers. Upon delivery they were thawed, amplified and frozen in working aliquots according to the suggestion of the suppliers. Cell lines were tested negative for mycoplasma contamination.

Mucilair™ human airway epithelia (HAE) are reconstituted epithelia composed with human primary cells at low passage (P₁) which are fully differentiated and functional. The HAE used in the present study have been reconstituted from primary cells of bronchial biopsies of a 56-year-old donor Caucasian female with no reported pathologies. They were maintained in air liquid interface with a serum free specific media (all from Epithelix SARL, Geneva, Switzerland, with informed consent).

Virus

SARS-CoV-2 strain BavPat1 was provided by Pr.Christian Drosten (Berlin, Germany) through European Virus Archive GLOBAL (<https://www.european-virus-archive.com/>). Inoculation with this strain at a MOI of 0.001, of a 25 cm² culture flask of confluent Vero E6 cells with MEM medium supplemented with 2.5% FBS, allowed us to prepare virus working stocks. Each 24h the cell supernatant medium was replaced in order to be harvested at the peak of infection. It was supplemented with 25mM HEPES (Sigma-Aldrich), aliquoted and stored at -80°C. Experiments with infectious virus were performed in a biosafety level 3 laboratory.

In vitro determination of EC₅₀ and CC₅₀

One day prior to infection, 96-well culture plates were seeded with 5×10⁴ Vero E6 or Caco-2 cells in 100μL assay medium per well (containing 2.5% FCS). The next day, eight 2-fold serial dilutions of compounds (from 20μM to 0.16μM for NTZ (BLDpharm) and from

100μM to 0.78μM for TIZ (MedChemExpress)) in triplicate were added to the cells (25μL/well, in assay medium). For the determination of the 50% and 90% effective concentrations (EC₅₀, EC₉₀; compound concentration required to inhibit by 50% or 90% viral RNA replication), four “virus control” wells were supplemented with 25μL of assay medium without any compounds. After 15min, a preset amount of virus diluted in 25μL of assay medium was added to the wells. This quantity of virus was calibrated so that the viral replication was still in the exponential growth phase for the readout, as previously described^{27–29} which correspond here to 150 TCID₅₀ per well. Four “cell control” wells were supplemented with 50μL of assay medium without any compounds or virus. On each culture plate, a positive control compound (Remdesivir, BLDpharm) was added in duplicate with eight 2-fold serial dilutions (0.16μM to 20μM). Plates were incubated for 2 days at 37°C prior to quantification of the viral genome by real-time RT-PCR as described below. For the determination of the 50% cytotoxic concentrations (CC₅₀; compound concentration required to reduce by 50% cell viability), the same culture conditions were used, without addition of the virus, and cell viability was measured using CellTiter Blue® (Promega) following manufacturer’s instructions. EC₅₀, EC₉₀ and CC₅₀ were determined using logarithmic interpolation as previously described.²⁸ The selectivity index of the compounds was calculated as the ratio of the CC₅₀ over the EC₅₀.

Ex vivo determination of antiviral activity

After being washed with pre-warmed OptiMEM medium (Life technologies), human airway epithelia were infected with SARS-CoV-2 at the apical side using a MOI of 0.1, as previously described (Pizzorno et al., 2020). Cells were cultivated in a basolateral medium that contained NTZ or remdesivir (positive control) at different concentrations or with no drug (virus control). Each day, medium was renewed and samples containing viral RNA were collected by washing the apical side with 200μL of pre-warmed OptiMEM medium. Four day after the infection, total intracellular RNA of each well was extracted using the RNeasy 96 HT kit (Qiagen) following manufacturer’s instructions. Viral RNA was quantified by RT-qPCR and infectious titers were determined in daily samples by TCID₅₀, both described below. *Ex vivo* experiments were approved by ethical committee and were conducted according to the declaration of Helsinki on biomedical research (Hong Kong amendment, 1989).

In vivo experiments

Approval and authorization. *In vivo* experiments were approved by the local ethical committee (C2EA—14) and the French ‘Ministère de l’Enseignement

Supérieur, de la Recherche et de l'Innovation' (APA-FIS#23975).

Animal handling. Three-week-old female Syrian hamsters were provided by Janvier Labs (SPF status). Animals were maintained in ISOcage P - Bioexclusion System (Techniplast) with unlimited access to water/food and 14h/10h light/dark cycle. A wooden gnawing block and extra bedding material was provided as cage enrichment. Animals were weighed and monitored daily for the duration of the study to detect the appearance of any clinical signs of illness/suffering. General anesthesia was obtained with isoflurane (Isoflurin®, Axience). Euthanasia, which was also realized under general anesthesia, was performed by cervical dislocation.

Study design. Group size was calculated with an effect size of 2 and a power of 80%, resulting in 5-6 animals/group. Sample sizes were maximized within the capacity of the BSL3 housing, and compound and virus stock availability. A total of 101 animals were used in this study. For the evaluation of antiviral activity of oral and intranasal treatment of NTZ (Figures 3, 5 and Supplementary Figure 2), groups of 6 animals were used (total number of 42, 12 and 12 hamsters respectively for data represented in Figures 3, 5 and Supplementary Figure 2). For the evaluation of lung histopathological changes (Figure 4), groups of 4 animals were used (total number of 8 hamsters). For the determination of plasma and lung concentrations of TIZ (Tables 1 and 2), groups of 3 and 6 animals were used (total number of 9 and 18 hamsters respectively for the single dose experiment and the multiple dose experiment). Animals were randomly assigned to groups but confounders were not controlled. Since, the same experimenters carried out infection/treatment/clinical follow-up, it was impossible to perform a blind trial. Blind trial were performed

NTZ dose (mg/kg)	C _{max} (µg/ml)	AUC _{0-24h} (µg·h/ml)
25.0	3.14	4.18
50.0	6.27	8.36
100	12.5	16.7
125	15.7	20.9
250	31.4	41.8
500	62.7	83.6

Table 2: Simulated pharmacokinetic parameters derived from nonlinear mixed-effect modelling using population mean values and median body weight of 0.126kg.

C_{max}: maximum plasma drug concentration; AUC_{0-24h}: area under the concentration-time curve from time 0 to 24h.

only for the evaluation of lung histopathological changes. Predefined humane endpoints (>20% weight loss, moribund and a scoring >10 calculated according to a clinical evaluation scale) were set as exclusion criteria. No animals were excluded from the study. For summary of the animal study design, a full ARRIVE list (Animal Research: Reporting of In Vivo Experiments) has been added as extra Supplementary Data file (<https://arriveguidelines.org>).

Hamster infection. After one week of acclimatisation, four-week-old anesthetized animals were intranasally infected with 50µL containing 10⁴ TCID₅₀ of virus in 0.9% sodium chloride solution. The mock-infected group was intranasally inoculated with 50 µL of 0.9% sodium chloride solution.

Drug preparation and administration. Hamsters were orally treated with either a NTZ solution at 10mg/mL, suspension at 27mg/mL or emulsion at 2.5mg/mL, prepared from NTZ powder (BLD Pharm). The solution was prepared with 0.5% of hydroxypropyl

	Time post-treatment	Plasma µg/mL	Lung µg/g	L/p ratio (%)
Single Dose: 13.5mg (control uninfected)	1 h	5.16 ± 4.24 (19.4 ± 16.0µM)	0.16 ; 0.22 § (0.61 ; 0.84µM/g)	4.8 ; 2.2
	2 h	3.39 ± 1.76 12.8 ± 6.62µM	0.13 ¶ (0.50µM/g)	2.7
	4 h	0.82 ± 0.57 (3.10 ± 2.16µM)	0.06 ¶ (0.23µM/g)	4.2
Multiple Dose: 500mg/kg/day BID (at 3 dpi)	12 h	0.94 ± 1.07 § (3.54 ± 4.21µM)	0.06 ; 0.06 § (0.21 ; 0.21µM/g)	2.7 ; 32.8
Multiple Dose: 750mg/kg/day TID (at 3 dpi)	12 hours	1.49 ± 1.15 (5.63 ± 4.35µM)	0.07 ; 0.16 § (0.28 ; 0.60µM/g)	2.9 ; 6.3

Table 1: Plasma and lung concentrations of TIZ after administration of a single dose or multiple dose of NTZ.

Multiple Dose: PK realized after 3 days of nitazoxanide administered two or three times a day, at the end of the dosing interval (trough concentrations). Data represent mean ± SD for plasma concentrations and individual values for lung concentrations and L/p ratios. These data represent a summary of Supplementary Data 5. Symbols §, ¶ and § represent respectively 1, 2 and 4 values below the limit of quantification.

methylcellulose and 0.1% of tween 80. For the suspension NTZ was dissolved in a vehicle composed of 90% (v/v) sterile distilled water, 7% (v/v) of tween 80 and 3% (v/v) ethanol 80%. The emulsion (aqueous/organic phase ratio of 80/20) for intranasal instillation was prepared with an aqueous phase (sterile distilled water 94% and absolute ethanol 6%) added gradually to an organic phase (NTZ 20mg/mL in cinnamaldehyde 75% and Kolliphore EL 25%) under constant stirring. A solution of favipiravir, reconstituted from anhydrous favipiravir (Toyama-Chemical) with 0.9% sodium chloride solution, was used for intra-peritoneally and intranasally treatment. Control group were orally or intranasally inoculated with a 0.9% sodium chloride solution.

Tissue collection. Lungs, nasal turbinates and blood were collected immediately after euthanasia. The left pulmonary lobe was first rinsed in 10mL of 0.9% sodium chloride solution, blotted with filter paper and weighed. Nasal turbinates and pulmonary lobes were transferred to a 2mL tube containing respectively 500µL or 1mL of 0.9% sodium chloride solution and 1mm or 3mm glass beads. They were crushed using a Tissue Lyser machine (Retsch MM400) for 5min at 30 cycles/s and then centrifuged 10 min at 16,200g. Crushed nasal tubinates were stored at -80°C while lung supernatant media were transferred to a 1.5mL tube, for another centrifugation during 10 min at 16,200g prior being stored at -80°C. One milliliter of blood was harvested in a 2mL tube containing 100µL of 0.5M EDTA (Life Technologies). Blood was centrifuged for 10 min at 16,200g and stored at -80°C.

Quantitative real-time RT-PCR (RT-qPCR) assays

All experiments were conducted in a molecular biology laboratory that is specifically devoted to molecular clinical diagnosis and which includes separate laboratories dedicated to each step of the procedure. Prior to PCR amplification, RNA extraction was carried out using the QIAamp 96 DNA kit and the Qiacube HT kit and the Qiacube HT (both from Qiagen) following the manufacturer's instructions. Shortly, 100µL of tissue clarified homogenates, spiked with 10µL of internal control (bacteriophage MS2), or viral supernatant were transferred into an S-block containing the recommended volumes of VXL, proteinase K and RNA carrier.

RT-qPCR (SARS-CoV-2 and MS2 viral genome detection) were performed with the GoTaq 1-step qRt-PCR kit (Promega) using 3.8µL of extracted RNA and 6.2µL of RT-qPCR mix that contains 250nM of each primer and 75nM of probe. Primers and probes sequences used are described in Supplementary Table 3. Quantification was provided by four 2 log serial dilutions of an appropriate T7-generated synthetic RNA standard of known quantities (10^2 to 10^8 copies/reaction).

Amplification was performed with the QuantStudio 12K Flex Real-Time PCR System (Applied Biosystems) using standard fast cycling parameters: 10min at 50°C, 2 min at 95°C, and 40 amplification cycles (95°C for 3 sec followed by 30sec at 60°C). qPCR (γ -actine gene detection) was performed under the same condition as RT-qPCR with the following modifications: we used the Express one step qPCR Universal kit (ThermoFisher Scientific) and the 50°C step of the amplification cycle was removed. Results were analyzed using QuantStudio 12K Flex Applied Biosystems software v1.2.3.

Tissue-culture infectious dose 50 (TCID₅₀) assay

To determine infectious titers, 96-well culture plates containing confluent Vero E6 cells were inoculated with 150µL per well of serial dilutions of each sample (ten-fold or four-fold dilutions when analyzing cell supernatant media or lung clarified homogenates respectively). Each dilution was performed in sextuplicate. After 5 days of incubation, plates were read for the absence or presence of cytopathic effect in each well. Infectious titers were estimated using the method characterized by Reed & Muench.³⁰

Nitazoxanide quantification in plasma and tissues

Quantification of TIZ in plasma and lung tissues was performed by high-performance liquid chromatography with UV detection method (Alliance 2695, Waters, USA) with a lower limit of quantification of 0.01µg/mL. The mobile phase consisted of 0.1% FA in water and 0.1% of FA in ACN (65:35, v/v). The chromatographic separation was achieved using an isocratic mode with an Xbridge BEH C18 2.5µm 4.6 × 100mm column. Peak area was quantified at 340nm using the Waters 2489 detector. TIZ was extracted by a simple protein precipitation method, using acetonitrile for plasma and ice-cold acetonitrile for clarified lung homogenates. Briefly, 200µL of samples matrix was added to 1000µL of acetonitrile solution containing the internal standard (thiopental), then vortexed for 2min followed by centrifugation for 10min at 4°C. The supernatant medium was evaporated under vacuum, then transferred to a 1.5mL Eppendorf tube. The dried residue was reconstituted with 100µL of ACN:water (50:50), vortexed for 30 seconds and centrifuged again for 10min at 4°C. The supernatant was transferred to an autosampler and 50µL was injected.

Histology

Animal handling, hamster infections, NTZ preparation and oral administrations were performed as described above. The anatomo-histological study was implemented as previously described.^{24,26} Briefly, lungs were collected after intratracheal instillation of 4% (w/v) formaldehyde solution, and then fixed 72h at room

temperature with a 4% (w/v) formaldehyde solution before being embedded in paraffin. Tissue sections of 3.5 μm were stained with hematoxylin-eosin (H&E) and blindly analyzed by a certified veterinary pathologist. Microscopic examination was done using a Nikon Eclipse E400 microscope. Different anatomic compartments were examined (1) for bronchial and alveolar walls, a score of 0 to 4 was assigned based on severity of inflammation; (2) regarding alveoli, a score of 0 to 2 was assigned based on presence and severity of hemorrhagic necrosis; (3) regarding vessel changes (leucocytic accumulation in vascular wall or in endothelial compartment), absence or presence was scored 0 or 1 respectively. A cumulative score was then calculated and assigned to a grade of severity (see Supplementary Table 4).

Pharmacokinetic modelling and simulation

NTZ is rapidly and completely hydrolyzed into its active metabolite TIZ.^{31,32} Therefore, the pharmacokinetic properties of NTZ were described using measured TIZ concentration in plasma.

At each time point, approximate 80 μl of blood were collected from the submandibular vein or the saphenous vein of hamsters. All samples were transferred into commercial K2-EDTA tubes, placed on ice until processed for plasma extraction by centrifugation and stored at -70°C before analysis. A LC-MS/MS-AI Triple Quad 5500 was used to determine TIZ concentrations. The mobile phase was a gradient of 0.1% formic acid (FA) in water and 0.1% of FA in acetonitrile (ACN), the column was an ACQUITY UPLC HSS T₃ 1.8 μm 2.1 \times 50mm. For mass spectrometry a positive electrospray ionization was used, and a selected reaction monitoring was set to select TIZ: [M+H]⁺+m/z: 266.0 / 121.2 and dexamethasone: [M+H]⁺+m/z: 393.0 / 373.1 as internal standard.

Pharmacokinetic profiles of TIZ in hamster were analyzed using a nonlinear mixed-effects modelling approach. The population pharmacokinetics analysis was performed using NONMEM[®] version 7.4. The final pharmacokinetic model was established by evaluating one-, two-, and three-compartment disposition models, as well as several different absorption models (i.e. first-order absorption, first-order absorption with lag time, and transit absorption models). The inter-individual variabilities of pharmacokinetic parameters were implemented as a log-normal distribution and the residual unexplained variability was modelled as an exponential error. Different doses of NTZ (i.e., 50, 100, 200, 500 and 1000mg/kg/day BID) were used to simulate TIZ exposures in hamsters (n=100) in order to compare to the simulated human exposure.

To simulate human PK profiles, a one-compartment model was used with pharmacokinetic parameters from an established PBPK model,³³ developed to describe pharmacokinetic data of TIZ plasma concentrations in

healthy individuals receiving single doses of 500–4000mg NTZ with/without food, presenting an apparent clearance of 19.34L/h and a volume of distribution of 38.68 L. The absorption was described with a first-order process and the rate constant (k_a) of 0.45h^{-1} was assumed in order to generate the mean concentration-time profile with a T_{max} at approximately 2 hours, as reported in healthy volunteers.³⁴ This model was used to simulate drug exposure at steady state in human after a dosing regimen of 1000mg/day BID of NTZ (the usual dose in humans), administered to 100 individuals. A total of 10 doses (5 days) were used for estimating the convergence rate to steady state.

All exposure simulations were performed in R version 4.0.4 using the mlxR package.³⁵

Graphical representations and statistical analysis

Graphical representations and statistical analyses were performed with Graphpad Prism 7 (Graphpad software). Two-sided statistical analysis were performed using Shapiro–Wilk normality test, Fisher's exact test, Student t-test, Mann–Whitney test, Welch's test, one-way and two-way ANOVA with Post-hoc Dunnett's multiple comparisons test. *P*-values lower than 0.05 were considered statistically significant. Statistical details for each experiment are described in the figure legends and in corresponding Supplementary Data. Experimental timelines were created on biorender.com.

Role of funders

The funders of the study had no role in study design, data collection, data analysis, data interpretation, writing of the report, or the decision to submit for publication. The corresponding author had full access to all data and had final responsibility for the decision to submit for publication.

Results

In vitro efficacy of nitazoxanide (NTZ)

Using two different cell lines, the Vero E6 (ACE2⁺/TMPRSS2⁻) and Caco-2 cells (ACE2⁺/TMPRSS2⁺), we first evaluated the *in vitro* efficacy of nitazoxanide (NTZ) and tizoxanide (TIZ) against SARS-CoV-2. Anti-viral potency was assessed in a viral RNA yield reduction assay by qRT-PCR as previously described.^{24–26,28,29} In Vero E6 cells, NTZ and TIZ inhibited viral replication with EC₅₀'s of 3.19 and 7.48 μM and EC₉₀'s of 10.27 and 9.27 μM , respectively, while both CC₅₀'s were above 60 μM (Figure 1). Selectivity Index (SI=CC₅₀/EC₅₀) were higher than 13.3 for both molecules. In Caco-2 cells, NTZ exhibited an EC₅₀ of 0.58 μM , an EC₉₀ of 1.75 μM and a CC₅₀ of 9.15 μM resulting in a SI of 15.8 (Figure 1).

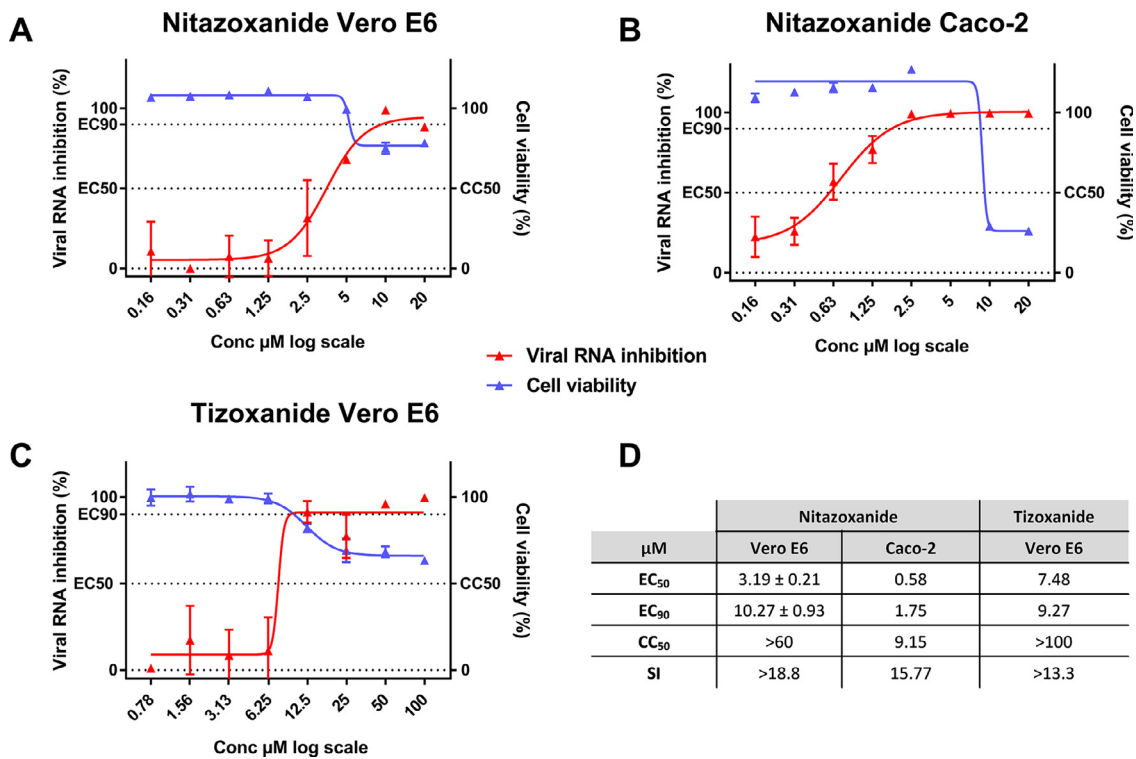


Figure 1. Antiviral activity of NTZ and TIZ in Vero E6 and Caco-2 cells.

Dose response curve and cell viability for: NTZ in Vero E6 (a) and Caco-2 (b) cells and for TIZ in Vero E6 cells (c). D: Table of EC₅₀, EC₉₀, CC₅₀. Results presented in the table for NTZ in Vero E6 are the mean ± SD from three independent experiments. Graphical representation is from one representative experiment.

Ex vivo efficacy of NTZ

We then investigated the *ex vivo* efficacy of NTZ using a recently described model of reconstituted human airway epithelial of bronchial origin.³⁶ Five different concentrations of NTZ (20; 10; 5; 2.5; 1.25 μM) were tested in duplicate while Remdesivir, at an active concentration of 10 μM, was used as a positive control. The basolateral sides of the epithelia were exposed to the drugs from time of infection until day 4 post infection (dpi). Media with fresh drug were renewed at 1, 2 and 3 dpi. Viral excretion was assessed at 2, 3 and 4 dpi, by measuring viral RNA yields and infectious titers at the apical side of the epithelium using quantitative real time RT-PCR and TCID₅₀ assays, respectively. No antiviral efficacy was detected when viral excretion was assessed by quantification of viral RNA (Figure 2-A). However, at 3 and 4 dpi, a significant reduction of infectious titers was observed when concentrations of NTZ above its EC₅₀ were used (with *p* values ranging from 0.01-0.05 for 5 μM, 0.001-0.01 for 10 μM and 0.0001-0.001 for 20 μM) (Figure 2).

In vivo efficacy of NTZ

Considering these results, we further investigated the potential antiviral activity of NTZ *in vivo* using a

previously described hamster model of SARS-CoV-2 infection.^{24-26,37}

Efficacy evaluation of a NTZ oral treatment. In a first set of experiments, we explored the antiviral efficacy of a NTZ suspension (90% sterile distilled water, 7% of tween 80 and 3% of ethanol 80%). During two independent experiments, groups of 6 hamsters were intranasally infected with 10⁴ TCID₅₀ of SARS-CoV-2 and received NTZ orally at doses of 500mg/kg/day BID or 750mg/kg/day TID (Figure 3a). Untreated groups of 6 hamsters received the suspension vehicle BID or TID. A group of 6 animals was treated with favipiravir (FVP) intraperitoneally (926mg/kg/day BID) as positive control in one experiment.²⁴

Hamsters treated with 500mg/kg/day BID or 750mg/kg/day TID of NTZ for 3 days (0, 1 and 2dpi), showed no significant differences for either infectious titers (measured using TCID₅₀ assay) or viral RNA yields (measured using quantitative real time RT-PCR assay) in clarified lung homogenates at 3 dpi compared to untreated animals (respectively for lung infectious titers and lung viral RNA yields : NTZ 500mg/kg/day BID : *p*=0.9933 and *p*=0.0989; NTZ 750mg/kg/day TID : *p*=0.5351 and *p*=0.3095) (Figures 3b, 3c, 3f and 3g).

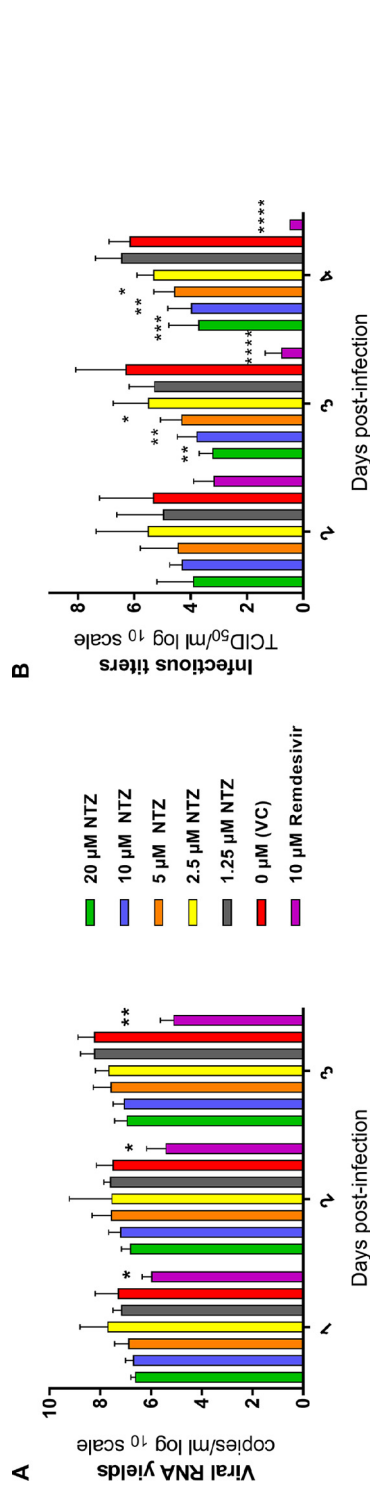


Figure 2. Antiviral activity of NTZ in a bronchial human airway epithelium. Kinetics of virus excretion at the apical side of the epithelium measured using an RT-qPCR assay (A) and a TCID₅₀ assay (B). Data represent mean ± SD. Statistical significance was calculated by Kruskal-Wallis test versus untreated group for (A) and 1-way ANOVA versus untreated group for (B). Remdesivir at 10μM was used as a positive drug control. *, **, *** and **** indicate and average significant value lower than that of the untreated group, with a p-value ranging between 0.01-0.05, 0.001-0.01, 0.0001-0.001 and <0.0001, respectively. Result are the mean ± SD of two independent experiment with in each experiment two independent inserts (Details in Supplementary Data 1).

No significant difference was detected with regards to viral RNA yields in plasma at 3 dpi (NTZ 500mg/kg/day BID: $p=0.4697$; NTZ 750mg/kg/day TID: $p=0.8672$) (Figures 3d and 3h). Administration of FVP, however, led as expected to significant reductions of both infectious titers and viral RNA yields in clarified lung homogenates (respectively for lung infectious titers and lung viral RNA yields: $p=0.0001$ and $p=0.0011$) (Figures 3b and 3c). NTZ-treated animals showed clinical signs of illness/suffering, with their mean normalized weight becoming significantly lower than that of untreated animals, at 3 dpi for animals treated with 500 mg/kg/day BID and at 2 dpi for animals treated with 750mg/kg/day TID ($p=0.0158$ and $p=0.0314$ respectively) (Figures 3e and 3i).

In another independent experiment, we tried to assess the antiviral efficacy of a longer treatment period. Despite receiving 500mg/kg/day of NTZ BID for 4 days (0, 1, 2 and 3 dpi), hamsters exhibited no significant reduction at 5 dpi of either infectious titers ($p=0.1775$) or viral RNA ($p=0.7003$) yields in their clarified lung homogenates, or viral RNA yields plasma ($p=0.1305$) (Figures 3j, 3k and 3l). However, they did not show any clinical signs of illness/suffering compared to untreated animals (Figure 3m).

We also explored the impact of NTZ treatment on lung pathological changes induced by SARS-CoV-2, in an independent experiment. Groups of 4 hamsters, intranasally infected with 10^4 TCID₅₀ of SARS-CoV-2, were orally treated at a dose of 500mg/kg/day BID for 4 days (0, 1, 2 and 3 dpi) (Figure 4a). Untreated hamsters (group of 4 animals) received the suspension vehicle BID. Animals were sacrificed at 5 dpi and a cumulative score from 0 to 10 (taking into account severity of inflammation, alveolar hemorrhagic necrosis and vessel lesions) was calculated and then assigned to a grade of severity (0=normal; 1=mild; 2=moderate; 3=marked and 4=severe; details in Supplementary Data 4). All animals, treated and untreated, displayed severe pulmonary impairments. Marked and severe histopathological damages in lungs for both groups were identified resulting in no significant difference of histopathological cumulative scores ($p=0.5601$) (Figure 4b). At 3 dpi, animals showed clinical signs of illness/suffering, with their mean normalized weight becoming significantly lower than that of untreated animals ($p=0.0175$) (Supplementary Figure 1).

To investigate if the lack of efficacy seen in lungs was due to an inadequate drug diffusion, we assessed the exposure and the lung distribution of TIZ (the active circulating metabolite of NTZ). We used tissues from infected animals sacrificed at 3 dpi following multiple administration (animals from Figure 3); an additional group of uninfected animals treated with a single dose of 13.5mg was used as control. TIZ concentration in plasma and in lung was quantified at 1, 2 and 4 hours post treatment for the single dose analysis (group of 3

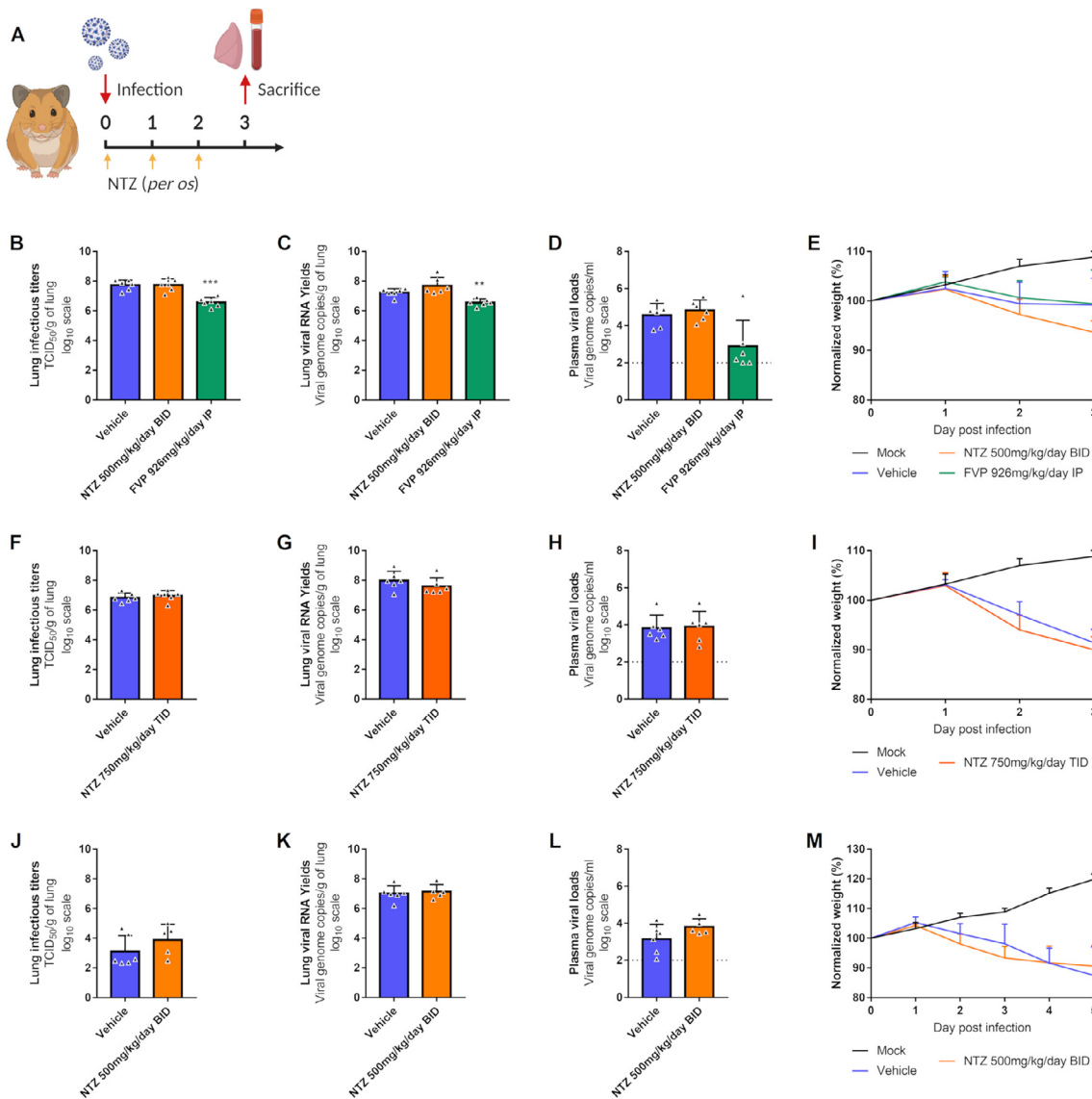


Figure 3. Antiviral activity of oral treatment of NTZ in a hamster model.

Groups of 6 hamsters were intranasally infected with 10^4 TCID₅₀ of virus. **a** Experimental timeline. **b, f, j** Viral replication in lung based on infectious titers (measured using a TCID₅₀ assay) expressed in TCID₅₀/g of lung ($n=6$ animals/group). **c, g, k** Viral replication in lung based on viral RNA yields (measured using an RT-qPCR assay) expressed in viral genome copies/g of lung ($n=6$ animals/group). **d, h, l** Plasma viral loads (measured using an RT-qPCR assay) are expressed in viral genome copies/mL of plasma (the dotted line indicates the detection threshold of the assay) ($n=6$ animals/group). **e, i, m** Clinical course of the disease ($n=6$ animals/group). Normalized weight at day n was calculated as follows: % of initial weight of the animal at day n . Data represent mean \pm SD (Details in Supplementary Data 2). Two-sided statistical analysis were performed using Shapiro–Wilk normality test, Fisher’s exact test, Student t-test, Mann–Whitney test and two-way ANOVA with Post-hoc Dunnett’s multiple comparisons test. *** and ** symbols indicate that the average value for the group is significantly lower than that of the untreated group with a p-value ranging between 0.0001–0.001 and 0.001–0.01 respectively (Details in Supplementary Data 2 and 3).

animals) and at 12 hours after the last administration for the multiple dose analysis (group of 6 animals).

These animals exhibited low penetration rates of TIZ in lungs, resulting in lung/plasma ratio ranging from 2.2% to 4.8% after single-dose administration (Table 1). Lung concentrations of TIZ were below the TIZ EC₅₀

found *in vitro* with Vero E6 cells (7.48 μ M, i.e. 1.98 μ g/mL), as well as effective NTZ concentrations *ex vivo* (5 μ M, i.e. 1.54 μ g/mL), and were not quantifiable in a total of 5 out of 9 animals (one at 1 hour, two at 2 hours and two at 4 hours) (Table 1). After 3 days of multiple dose treatment, TIZ trough concentrations (12 hours after

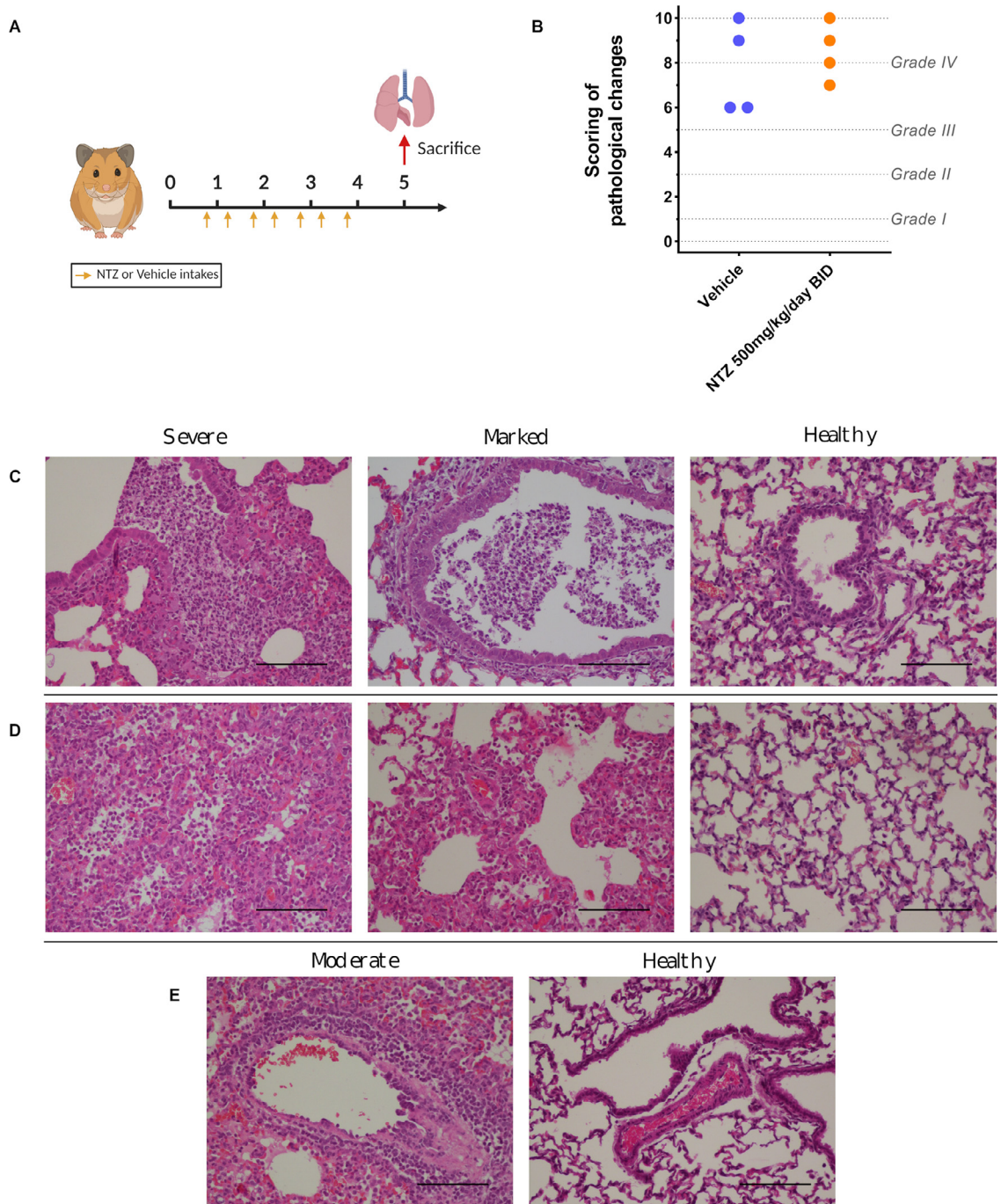


Figure 4. Lung histopathological changes.

Groups of 4 animals were intranasally infected with 10^4 TCID₅₀ of virus and sacrificed at 5 dpi. Based on severity of inflammation, alveolar hemorrhagic necrosis and vessel lesions, a cumulative score from 0 to 10 was calculated and assigned to a grade of severity (I, II, III and IV). **a** Experimental timeline. **b** Scoring of pathological changes (Details in Supplementary Data 4). Two-sided statistical analysis was performed using Shapiro–Wilk normality test, Fisher's exact test, and Student t-test. **c** Representative images of bronchial inflammation (scale bar: 100 μ): severe peribronchiolar inflammation and bronchiole filled with numerous neutrophils, marked peribronchiolar inflammation and normal bronchi. **d** Representative images of alveolar inflammation (scale bar: 100 μ): severe infiltration of alveolar walls, alveoli filled with neutrophils/macrophages, marked infiltration of alveolar walls, some alveoli filled with neutrophils/macrophages and normal alveoli. **e** Representative images of vessel inflammation (scale bar: 100 μ): moderate accumulation of inflammatory cells in arteriolar walls and normal arteriole.

the last administration) in lungs were still below the *in vitro* EC₅₀ and not quantifiable in a total of 8 out of 12 animals (four for each multiple dose concentration) (Table 1).

NTZ efficacy evaluation following intranasal administration. To assess other administration routes for NTZ, we explored the antiviral efficacy of an intranasal NTZ emulsion (aqueous phase: sterile distilled water 94% and absolute ethanol 6%; organic phase: NTZ 20mg/mL in cinnamaldehyde 75% and Kolliphore EL 25%). Hamsters were intranasally infected with 10⁴ TCID₅₀ of SARS-CoV-2. A group of 6 hamsters received intranasally 2.8mg/kg/day TID of NTZ (Figure 5a). An untreated group of 6 hamsters received the emulsion vehicle TID. All treatments were started at the day of infection and ended at day 2 post infection. Viral replication was assessed in lungs, plasma and nasal turbinates at 3 dpi.

NTZ intranasal treatment led to a significant increase of infectious titers in clarified lung homogenates ($p=0.0003$) (Figure 5b). No significant differences were observed when looking at viral RNA yields in both clarified lung homogenates and plasma ($p=0.4530$ and $p=0.5232$ respectively) (Figure 5c and 5d). In nasal turbinates, no significant differences of infectious titers were observed between the groups ($p=0.6295$) (Figure 5e). When looking at viral RNA yields, NTZ treatment induced a significant reduction of viral RNA load in nasal turbinates ($p=0.0037$) (Figure 5f). Animals treated with NTZ intranasally from 1 to 3 dpi, showed clinical signs of illness/suffering, with their mean normalized weight becoming significantly lower than that of untreated animals ($p=0.0001$) (Figure 5g).

To confirm these results, the experiment was repeated independently. Overall, no significant differences in viral replication between treated and untreated hamsters were observed in either clarified lung homogenates, plasma or nasal turbinates (lung infectious titers : $p=0.9846$; lung viral RNA yields : $p=0.7366$; plasmatic viral loads : $p=0.2475$; nasal turbinate's infectious titers : $p=0.1133$; nasal turbinate's viral RNA yields : $p=0.13406$) (Supplementary Figure 2). Once again, hamsters treated with NTZ intranasally from 1 to 3 dpi, showed clinical signs of illness/suffering, with their mean normalized weight becoming significantly lower than that of untreated animals ($p=0.0004$ at 1 dpi; $p=0.0001$ at 2 and 3 dpi) (Supplementary Figure 2).

Similarly to the oral administration study, and to investigate a potential issue regarding drug distribution to the compartment of choice, we also assessed the plasma, lung and nasal turbinates concentrations of TIZ following intranasal NTZ administration in infected animals treated by multiple doses, 12 hours after the last administration (group of 6 hamsters from Figure 5). Overall, TIZ was detectable in only 2 out of 6 animals (one in plasma and lung ; one in lung and nasal turbinates) (Supplementary Table 1) but TIZ

concentrations were below the EC₅₀ found *in vitro* and the active concentration *ex vivo*.

Pharmacokinetic modelling. We characterized the pharmacokinetic profile of TIZ in hamster after administration of the same NTZ suspension or TIZ formulated in 10% [Tween 80, 80% EtOH (70:30 v/v)] and 90% distilled water, homogenous opaque suspension. Groups of 3 hamsters received an oral single dose of 485mg/kg, 98.1mg/kg or 25.5mg/kg of NTZ or 96.4mg/kg of TIZ. The corresponding concentration-time curves for NTZ administration only are presented in Supplementary Figure 3. Notably, similar concentration-time curves of TIZ were observed following oral administration of 98.1 NTZ or 96.4mg/kg of TIZ, suggesting full in-vivo conversion of NTZ into TIZ (Supplementary Figure 3). The observed TIZ plasma concentration-time data in hamster, following oral administration of NTZ and TIZ, were characterized using nonlinear mixed-effects modelling. The data were best described by a two-compartment disposition model with first-order absorption. The population pharmacokinetic parameters estimates from the final model are presented in Supplementary Table 2. Time to maximum concentration (T_{max}) and terminal elimination half-life ($t_{1/2}$) were estimated to 0.276h and 0.80h, respectively. Graphically, the model showed good adequacy between predicted concentrations and observed concentrations (Supplementary Figure 4).

Simulated secondary pharmacokinetic parameters (C_{max} and AUC_{0-24h}) at each NTZ dose derived from the population pharmacokinetic model are presented in Table 2.

We then compared the pharmacokinetic profile of TIZ in hamster to the one at steady state in human. The pharmacokinetic model developed to describe the TIZ concentration-time data in hamster was used to simulate plasma drug exposures in hamster using different dose regimens. From these simulations, TIZ C_{max} , AUC (AUC at steady state over 1 dosing interval) and C_{min} were derived and compared to simulated plasma PK parameters in human using a published physiologically-based pharmacokinetic (PBPK) model.³³ A dose between 50 and 100mg/kg/day BID in hamsters provided C_{max} values close to that obtained in humans after a dose of 1000mg/day BID (the usual dose in humans). A dose between 200 and 500mg/kg BID in hamster provided AUC values quite similar to the one obtained in humans. However, human C_{min} was never reached at any dose in hamsters (Figure 6).

Discussion

Nitazoxanide was among the very first molecules studied at the beginning of the COVID-19 pandemic, revealing an *in vitro* antiviral efficacy against SARS-CoV-

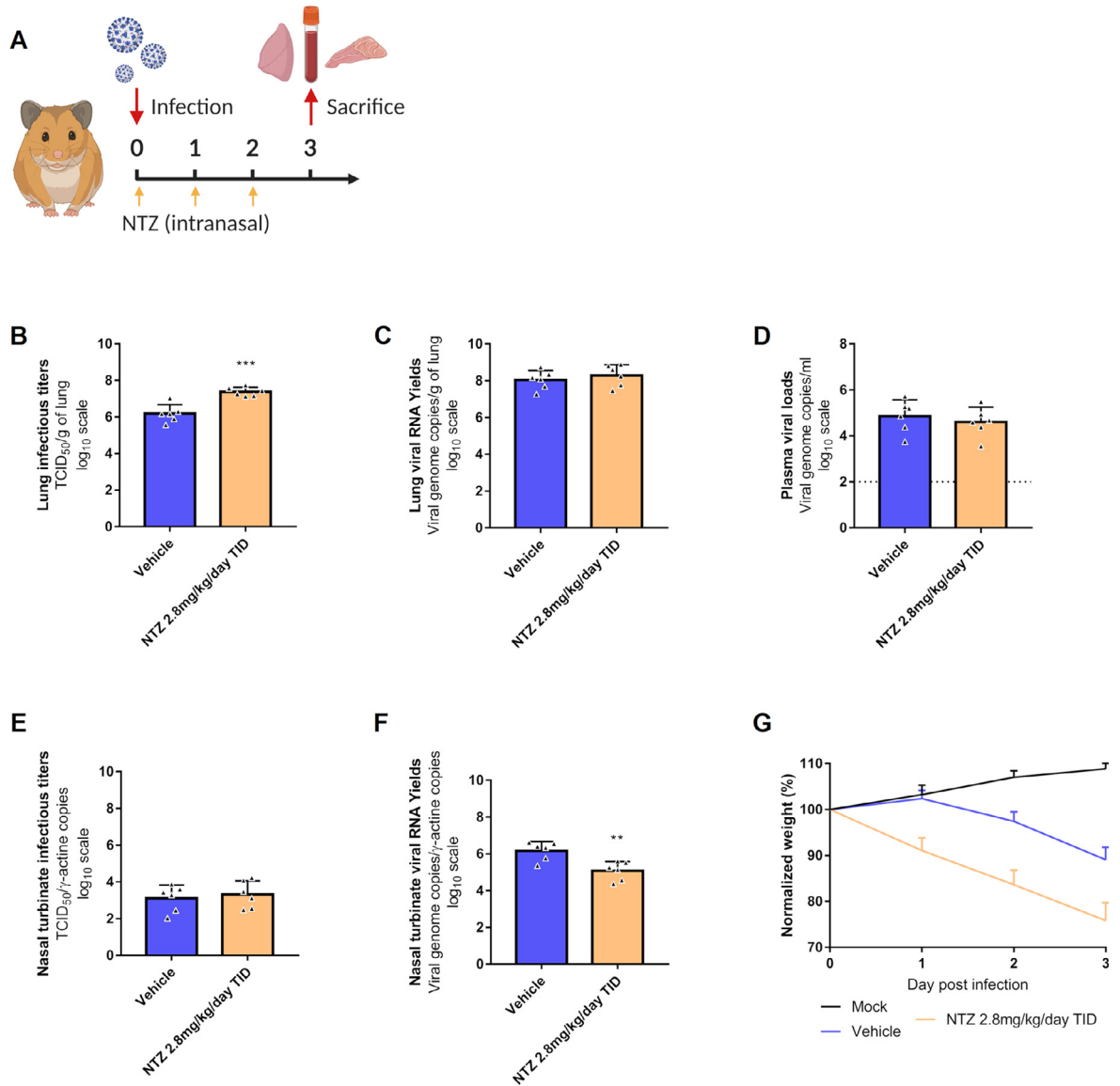


Figure 5. Antiviral activity of intranasal treatment of NTZ in a hamster model.

Groups of 6 hamsters were intranasally infected with 10^4 TCID₅₀ of virus. **a** Experimental timeline. **b** Viral replication in lung based on infectious titers (measured using a TCID₅₀ assay) expressed in TCID₅₀/g of lung ($n=6$ animals/group). **c** Viral replication in lung based on viral RNA yields (measured using an RT-qPCR assay) expressed in viral genome copies/g of lung ($n=6$ animals/group). **d** Plasma viral loads (measured using an RT-qPCR assay) are expressed in viral genome copies/mL of plasma (the dotted line indicates the detection threshold of the assay) ($n=6$ animals/group). **e** Viral replication in nasal turbinates based on infectious titers (measured using a TCID₅₀ assay) expressed in TCID₅₀/copy of γ -actine gene ($n=6$ animals/group). **f** Viral replication in nasal turbinates based on viral RNA yields (measured using an RT-qPCR assay) expressed in viral genome copies/copy of γ -actine gene ($n=6$ animals/group). **g** Clinical course of the disease ($n=6$ animals/group). Normalized weight at day n was calculated as follows: % of initial weight of the animal at day n . Data represent mean \pm SD (Details in Supplementary Data 2). Two-sided statistical analysis were performed using Shapiro–Wilk normality test, Fisher’s exact test, Student t-test and two-way ANOVA with Post-hoc Dunnett’s multiple comparisons test. ** symbols indicate that the average value for the group is significantly lower than that of the untreated group with a p -value ranging between 0.001-0.01 (Details in Supplementary Data 2 and 3).

2.9.14–21 Our study confirms these results, as we found that NTZ possesses EC₅₀ under $5\mu\text{M}$ in two different cell lines. In addition, we demonstrated that NTZ was

active in bronchial human airway epithelia, which largely mimic the structural, functional, and innate immune features of the human respiratory epithelium,

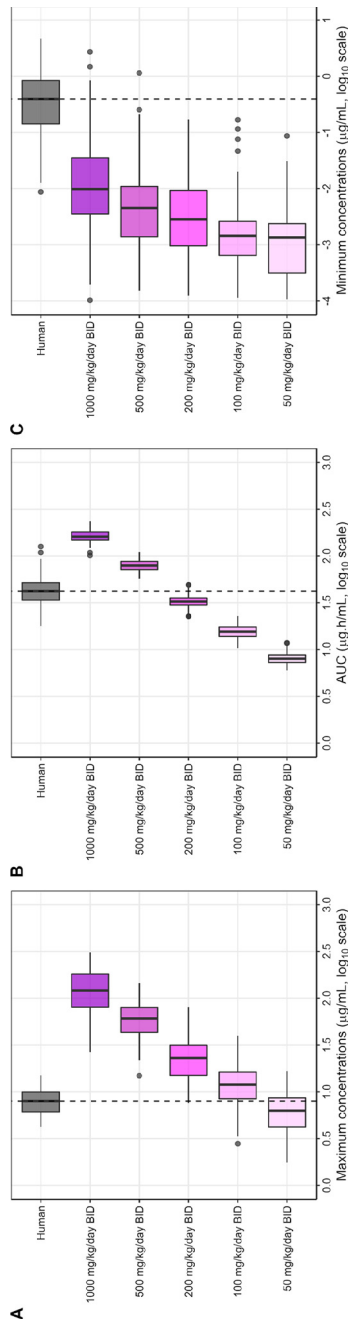


Figure 6. Simulated pharmacokinetic parameters of TIZ in human and hamster at steady state. Predicted steady-state pharmacokinetic parameters of TIZ, i.e. C_{max} (A), AUC (B) and C_{min} (C), in human associated with receiving 1000mg/day BID of NTZ (grey box) were compared with pharmacokinetic parameters of hamster receiving 50, 100, 200, 500 and 1000mg/kg/day BID of NTZ (colored boxes). Boxes and whiskers represent the median with inter-quantile range and the 95% prediction intervals, respectively.

albeit at lower potency as compared to Remdesivir, the positive control in this assay.³⁶

It is well documented that, *in vivo*, NTZ is rapidly deacetylated to its active metabolite, TIZ.³¹ However, only one non-peer-reviewed source reported the activity of TIZ against SARS-CoV-2 (<https://opendata.ncats.nih.gov/covid19/databrowser>). Here, we demonstrated that this metabolite is indeed active against SARS-CoV-2 *in vitro* with an EC_{50} of 7.48µM, reinforcing the potential use of NTZ in COVID-19 management.

Although mainly considered as an antiprotozoal agent, NTZ, and its active circulating TIZ metabolite, were identified as *in vitro* broad-spectrum antiviral compounds, since they both inhibit the replication of a wide range of RNA and DNA viruses in cell culture.^{6,9} Their antiviral mechanism has not been clearly elucidated. However, it seems that interaction with numerous targets implicated in viral pathogenesis, depending on the virus, is involved (immunomodulatory effects and direct drug action)⁹ Notably, post-entry inhibition by upregulation of cell's innate antiviral response, observed against hepatitis C virus on cell culture,³⁸ may be one of the efficient antiviral pathways involved in SARS-CoV-2 inhibition. Recently, TMEM16 inhibitors, such as niclosamide and NTZ, have been reported to protect against cell fusion induced by SARS-CoV-2 spike protein in cell culture.²² This syncytia inhibition could be one of the modes of action observed *in vitro* and *ex vivo* for NTZ antiviral activity against SARS-CoV-2.

Although NTZ has had only incomplete preclinical characterization, numerous clinical trials using the molecule are underway around the world. We felt that the generation of robust preclinical data was relevant to document the suitability of NTZ for clinical use in the treatment of COVID patients.

Despite promising *in vitro* results and new hypotheses on its antiviral mechanism, NTZ failed to reduce the severity of SARS-CoV-2 infection *in vivo* in the Syrian hamster model. No significant improvement in terms of clinical course of the disease, viral replication (based on infectious titers or viral RNA yields) and/or histopathological damages in lungs was observed when using two different dosing regimens of NTZ. These findings could be explained by the insufficient pulmonary diffusion of TIZ, since peak concentrations in lungs (1 hour post-treatment) never exceeded its *in vitro* or *ex vivo* EC_{50} . This insufficient pulmonary exposure was confirmed by the low accumulation of TIZ over time in the lungs as trough concentrations after 3 days of multiple doses of NTZ were similar to those found 4 hours post-treatment in the single dose model. This result is in accordance with a previous clinical trial assessing the safety, bactericidal activity, and pharmacokinetics of NTZ in adults with pulmonary tuberculosis, where sputum concentration of NTZ was low, suggesting that it did not penetrate pulmonary lesions to a sufficient degree.³⁹ This can be explained in part by the

physico-chemical and pharmacokinetic characteristics of the product, which do not facilitate tissue diffusion. In addition to being a moderately lipophilic molecule, TIZ is highly bound to plasma proteins (99%). Therefore, the use of NTZ as a systemic treatment might be challenging.

The PK modeling and simulations provided further insights for the lack of NTZ efficacy in the *in vivo* hamster model of SARS-CoV-2 infection. Simulations showed that the dose of 500mg/kg/day BID (found ineffective in our study) was sufficient to achieve C_{max} and AUC above those observed in humans at the usual dose of 1000mg/day, but not sufficient to reach trough concentrations (C_{min}) observed in humans at this same dose. Furthermore, human C_{min} was never reached even with the highest simulated dose in hamsters (1000mg/kg/day BID). This prediction was confirmed in our *in vivo* study in which we did not observe efficacy at the highest dose (*i.e.* 750mg/kg/day TID). The latter observations show a difference in the clearance of NTZ between humans and hamsters, of which the C_{min} can be considered a reflection, with a more rapid elimination in hamsters. Although differences in pharmacokinetic profiles between humans and hamsters are known and widely documented, these findings suggest that at the usual dose of 1000mg/day in humans, NTZ will have no effect on SARS-CoV-2 replication.

To potentially enhance the pulmonary diffusion and explore the possible antiviral activity of TIZ within the upper respiratory tract, hamsters were treated with an intranasal NTZ emulsion formulation. This alternative route of administration proved ineffective in our model, as no significant improvement in any of the disease endpoints analysed was observed. As observed after oral administration, TIZ trough concentration measured in lungs after 3 days of intranasal NTZ administration was very low, which may also partly explain the lack of antiviral efficacy; in all samples tested, including nasal turbinates, TIZ concentration was found to be well below the *in vitro* and *ex vivo* EC_{50} . This lack of TIZ accumulation in the upper respiratory tract should be interpreted with caution as no active intranasal deliverable compounds was available as a positive control in our study.

Overall, this work reinforces the need for multidisciplinary preclinical studies prior to conducting human clinical trials: based on the pharmacokinetic data collected in this pre-clinical study, the use of NTZ as an antiviral against SARS-CoV-2, does not seem appropriate at the current standard formulation and dosage. It would appear that this issue has been taken into account recently as a large majority of previous and currently ongoing trials use/have used higher doses of NTZ than usually recommended, as in the ANTICOV trial COVERAGE Africa^{40,41} (<https://clinicaltrials.gov/>). Our results suggest that the low pulmonary bioavailability of NTZ remains the major challenge that needs to be

addressed in order to properly evaluate the potential antiviral effect of NTZ in an animal model or in human.

The outcomes of the current clinical trials will be very useful for back-translation purposes. As an example, if preliminary data of a recent trial may suggest that NTZ could have some beneficial impact in preventing worsening of the disease and need for hospitalization, qualitative and quantitative tests to detect SARS-CoV-2 were not significantly different between the treatment arms.⁴² These observations corroborate our results and demonstrate that it will be essential to increase the pulmonary bioavailability of NTZ in order to conclude a direct antiviral impact.

In conclusion, optimization of the NTZ formulation may allow reconsideration of the potential use of the drug for the treatment of SARS-CoV-2 infection. In a previous pharmacokinetic study of NTZ in mice, optimal concentrations of TIZ were obtained in the lungs when the molecule was entrapped in inhalable particles.⁴³ This type of formulation combined with aerosol administration could potentially lead to an effective concentration of NTZ in the animal's lungs and deserves further investigation.

Limitations of the study

In this work, we focused mainly on the evaluation of the direct antiviral activity of NTZ against SARS-CoV-2. Regarding its indirect activity, we evaluated the animals clinically and the impact of the treatment on the histopathology of the lungs. When treated with NTZ, these two clinical endpoints were not improved, indicating that the indirect antiviral actions of NTZ were not achieved at the doses used. Some studies have shown that NTZ and its active metabolite, TIZ, have the ability to inhibit the production of pro-inflammatory cytokines (TNF-alpha, interleukins, chemokines, etc.) and to induce host-directed antiviral mechanisms, including interferon-stimulated gene expression. Thus, one of the limitations of our study is that we did not measure the expression of all these markers.

On the other hand, this study was only conducted with an ancestral strain of SARS-CoV-2, the BavPat1 strain. The evaluation of the activity of NTZ on new variants of SARS-CoV-2 could be interesting, especially concerning the clinical and immunomodulatory aspects, since these criteria can evolve according to the variant.

Contributors

All authors read and approved the final version of the manuscript.

Conceptualization, J.S.D., F.T., R.H., J.T., F.E., I.S., E.C., C.S. and A.N.; methodology, J.S.D., F.T., R.H., J.T., F.E., I.S., E.C., C.S. and A.N.; formal analysis, J.S.D., M.C., F.T., C.L. T.W. and P.C.; investigation, J.S.D., M.C.,

F.T., P.R.P., M.G., G.M., K.B., C.L., T.W., P.C., C.S. and A.N.; resources, F.E., I.S., E.C., X.d.L., C.S. and A.N.; writing—original draft, J.S.D., F.T., T.W., P.C., C.S. and A.N.; writing—review & editing, C.L., R.H., J.T., F.E., I.S., E.C., X.d.L., C.S. and A.N.; visualization, J.S.D., M.C., F.T., P.R.P., T.W., P.C. and A.N.; supervision, F.E., I.S., E.C. and A.N.; funding acquisition, F.E., I.S., E.C., X.d.L., C.S. and A.N.

Data sharing statement

All of the data generated or analyzed during this study are included in this published article. All data supporting the findings in this study are also available from the corresponding author upon request.

Declaration of interests

None to declare.

Acknowledgements

We thank Laurence Thirion (UVE; Marseille) for providing RT-qPCR systems. We thank Camille Placidi (UVE; Marseille) for her technical contribution. We thank Pr Drosten and Pr Drexler for providing the SARS-CoV-2 strain through the European Research infrastructure EVA GLOBAL. We thank Toyama-Chemical Favipiravir for kindly providing the favipiravir. This work was supported by the Fondation de France “call FLASH COVID-19”, project TAMAC, by “Institut national de la santé et de la recherche médicale” through the REACTing (REsearch and ACTion targeting emerging infectious diseases), by REACTING/ANRS MIE under the agreement No. 21180 (‘Activité des molécules antivirales dans le modèle hamster’), by European Virus Archive Global (EVA 213 GLOBAL) funded by the European Union’s Horizon 2020 research and innovation program under grant agreement No. 871029 and DNDi under support by the Wellcome Trust Grant ref: 222489/Z/21/Z through the COVID-19 Therapeutics Accelerator”. Part of this work was supported by the Wellcome Trust [220211]. Part of the work was done on the Aix Marseille University antivirals platform “AD2P”. For the purpose of open access, the author has applied a CC BY public copyright licence to any Author Accepted Manuscript version arising from this submission.

Supplementary materials

Supplementary material associated with this article can be found in the online version at doi:10.1016/j.ebiom.2022.104148.

References

- Zhu N, Zhang D, Wang W, et al. A novel coronavirus from patients with pneumonia in China, 2019. *N Engl J Med.* 2020;382(8):727–733.

- Zhou P, Yang XL, Wang XG, et al. A pneumonia outbreak associated with a new coronavirus of probable bat origin. *Nature.* 2020;579(7798):270–273.
- WHO. World Health Organization. WHO Director-General’s opening remarks at the media briefing on COVID-19 - 11 March 2020. Available from: <https://www.who.int/director-general/speeches/detail/who-director-general-s-opening-remarks-at-the-media-briefing-on-covid-19-11-march-2020>.
- Le Bert N, Tan AT, Kunasegaran K, et al. SARS-CoV-2-specific T cell immunity in cases of COVID-19 and SARS, and uninfected controls. *Nature.* 2020;584(7821):457–462.
- Kratky M, Vinsova J. Antiviral activity of substituted salicylanilides—a review. *Mini Rev Med Chem.* 2011;11(11):956–967.
- Rossignol JF. Nitazoxanide: a first-in-class broad-spectrum antiviral agent. *Antiviral Res.* 2014;110:94–103.
- Mahmoud DB, Shitu Z, Mostafa A. Drug repurposing of nitazoxanide: can it be an effective therapy for COVID-19? *J Genet Eng Biotechnol.* 2020;18(1):35.
- Cao J, Forrest JC, Zhang X. A screen of the NIH clinical collection small molecule library identifies potential anti-coronavirus drugs. *Antiviral Res.* 2015;114:1–10.
- Stachulski AV, Taujanskas J, Pate SL, et al. Therapeutic potential of nitazoxanide: an appropriate choice for repurposing versus SARS-CoV-2? *ACS Infect Dis.* 2021;7(6):1317–1331.
- Beigel JH, Nam HH, Adams PL, et al. Advances in respiratory virus therapeutics - a meeting report from the 6th isriv Antiviral Group conference. *Antiviral Res.* 2019;167:45–67.
- Rossignol JF. Nitazoxanide, a new drug candidate for the treatment of Middle East respiratory syndrome coronavirus. *J Infect Public Heal.* 2016;9(3):227–230.
- Rossignol JF, La Frazia S, Chiappa L, Ciucci A, Santoro MG. Thiazolidines, a new class of anti-influenza molecules targeting viral hemagglutinin at the post-translational level. *J Biol Chem.* 2009;284(43):29798–29808.
- Belardo G, Cenciarelli O, La Frazia S, Rossignol JF, Santoro MG. Synergistic effect of nitazoxanide with neuraminidase inhibitors against influenza A viruses in vitro. *Antimicrob Agents Chemother.* 2015;59(2):1061–1069.
- Martins PR, Barreto-Alves JA, Fakhouri R. Potential role for nitazoxanide in treating SARS-CoV-2 infection. *Am J Physiol-Lung C.* 2020;319(1):L35–L36.
- Chibber P, Haq SA, Ahmed I, Andrabi NI, Singh G. Advances in the possible treatment of COVID-19: A review. *Eur J Pharmacol.* 2020;883:173372.
- Alonso DF, Farina HG. Repurposing of host-based therapeutic agents for the treatment of coronavirus disease 2019 (COVID-19): a link between antiviral and anticancer mechanisms? *Int J Antimicrob Agents.* 2020;56(3):106125.
- Dos Santos WG. Natural history of COVID-19 and current knowledge on treatment therapeutic options. *Biomed Pharmacother.* 2020;129:110493.
- Yang CW, Peng TT, Hsu HY, et al. Repurposing old drugs as antiviral agents for coronaviruses. *Biomed J.* 2020;43(4):368–374.
- Arshad U, Pertinez H, Box H, et al. Prioritization of anti-SARS-CoV-2 drug repurposing opportunities based on plasma and target site concentrations derived from their established human pharmacokinetics. *Clin Pharmacol Ther.* 2020;108(4):775–790.
- Wang M, Cao R, Zhang L, et al. Remdesivir and chloroquine effectively inhibit the recently emerged novel coronavirus (2019-nCoV) in vitro. *Cell Res.* 2020;30(3):269–271.
- Mostafa A, Kandeil A, AMME Y, et al. FDA-approved drugs with potent in vitro antiviral activity against severe acute respiratory syndrome coronavirus 2. *Pharmaceuticals (Basel).* 2020;13(12):443.
- Braga L, Ali H, Secco I, et al. Drugs that inhibit TMEM16 proteins block SARS-CoV-2 spike-induced syncytia. *Nature.* 2021;594(7861):88–93.
- Lokhande AS, Devarajan PV. A review on possible mechanistic insights of Nitazoxanide for repurposing in COVID-19. *Eur J Pharmacol.* 2021;891:173748.
- Driouich JS, Cochin M, Lingas G, et al. Favipiravir antiviral efficacy against SARS-CoV-2 in a hamster model. *Nat Commun.* 2021;12(1):1735.
- Touret F, Driouich JS, Cochin M, et al. Preclinical evaluation of Imatinib does not support its use as an antiviral drug against SARS-CoV-2. *Antiviral Res.* 2021;193:105137.
- Cochin M, Touret F, Driouich JS, et al. Hydroxychloroquine and azithromycin used alone or combined are not effective against

- SARS-CoV-2 ex vivo and in a hamster model. *Antiviral Res.* 2022;197:105212.
- 27 Delang L, Li C, Tas A, et al. The viral capping enzyme nsP1: a novel target for the inhibition of chikungunya virus infection. *Sci Rep-Uk.* 2016;6:31819.
- 28 Touret F, Baronti C, Goethals O, Van Look M, de Lamballerie X, Querat G. Phylogenetically based establishment of a dengue virus panel, representing all available genotypes, as a tool in dengue drug discovery. *Antiviral Res.* 2019;168:109–113.
- 29 Touret F, Gilles M, Barral K, et al. In vitro screening of a FDA approved chemical library reveals potential inhibitors of SARS-CoV-2 replication. *Sci Rep.* 2020;10(1):13093.
- 30 LJaMH Reed. A simple method of estimating fifty per cent endpoint. *Am J Epidemiol.* 1938;27(3):493–497.
- 31 Broekhuysen J, Stockis A, Lins RL, De Graeve J, Rossignol JF. Nitazoxanide: pharmacokinetics and metabolism in man. *Int J Clin Pharmacol Ther.* 2000;38(8):387–394.
- 32 Harausz EP, Chervenak KA, Good CE, et al. Activity of nitazoxanide and tizoxanide against *Mycobacterium tuberculosis* in vitro and in whole blood culture. *Tuberculosis (Edinb).* 2016;98:92–96.
- 33 Rajoli RKR, Pertinez H, Arshad U, et al. Dose prediction for repurposing nitazoxanide in SARS-CoV-2 treatment or chemoprophylaxis. *Br J Clin Pharmacol.* 2021;87(4):2078–2088.
- 34 Balderas-Acta JI, Rios-Rodríguez Bueno EP, Pérez-Becerril F, Espinosa-Martínez C, Burke-Fraga V, González-de la Parra G. Bioavailability of two oral-suspension formulations of a single dose of nitazoxanide 500 mg: an open-label, randomized-sequence, two-period crossover, comparison in healthy fasted Mexican adult volunteers. *J Bioequiv Availab.* 2011;3(3):043–047.
- 35 Lavielle M mlxR: Simulation of Longitudinal Data. 2017.
- 36 Pizzorno A, Padey B, Julien T, et al. Characterization and treatment of SARS-CoV-2 in nasal and bronchial human airway epithelia. *Cell Rep Med.* 2020;1(4):100059.
- 37 Chan JF, Zhang AJ, Yuan S, et al. Simulation of the clinical and pathological manifestations of coronavirus disease 2019 (COVID-19) in a golden syrian hamster model: implications for disease pathogenesis and transmissibility. *Clin Infect Dis.* 2020;71(9):2428–2446.
- 38 Elazar M, Liu M, McKenna SA, et al. The anti-hepatitis C agent nitazoxanide induces phosphorylation of eukaryotic initiation factor 2alpha via protein kinase activated by double-stranded RNA activation. *Gastroenterology.* 2009;137(5):1827–1835.
- 39 Walsh KF, McAulay K, Lee MH, et al. Early bactericidal activity trial of nitazoxanide for pulmonary tuberculosis. *Antimicrob Agents Chemother.* 2020;64(5):e01956-19.
- 40 Blum VF, Cimerman S, Hunter JR, et al. Nitazoxanide superiority to placebo to treat moderate COVID-19 - a pilot prove of concept randomized double-blind clinical trial. *EClinicalMedicine.* 2021;37:100981.
- 41 Rocco PRM, Silva PL, Cruz FF, et al. Early use of nitazoxanide in mild COVID-19 disease: randomised, placebo-controlled trial. *Eur Respir J.* 2021;58(1):2003725.
- 42 Rossignol JF, Bardin MC, Fulgencio J, Mogelnicki D, Brechot C. A randomized double-blind placebo-controlled clinical trial of nitazoxanide for treatment of mild or moderate COVID-19. *EClinicalMedicine.* 2022;45:101310.
- 43 Gupta A, Tulsankar SL, Bhatta RS, Misra A. Pharmacokinetics, metabolism, and partial biodistribution of “pincer therapeutic” nitazoxanide in mice following pulmonary delivery of inhalable particles. *Mol Pharm.* 2017;14(4):1204–1211.